Chaos

Central pattern generator based on self-sustained oscillator coupled to a chain of oscillatory circuits

Cite as: Chaos **32**, 033117 (2022); https://doi.org/10.1063/5.0077789
Submitted: 06 November 2021 • Accepted: 28 February 2022 • Published Online: 17 March 2022

Semen A. Kurkin, Danil D. Kulminskiy, Vladimir I. Ponomarenko, et al.

Chaos ARTICLE scitation.org/journal/cha

Central pattern generator based on self-sustained oscillator coupled to a chain of oscillatory circuits

Cite as: Chaos 32, 033117 (2022); doi: 10.1063/5.0077789
Submitted: 6 November 2021 · Accepted: 28 February 2022 ·
Published Online: 17 March 2022

View Online Export Citation CrossMark

Semen A. Kurkin,[1,2] Danil D. Kulminskiy,[3,4] Vladimir I. Ponomarenko,[4] Mikhail D. Prokhorov,[4] Sergey V. Astakhov,[5] and Alexander E. Hramov[1,2,4,a)]

AFFILIATIONS

[1]Immanuel Kant Baltic Federal University, Kaliningrad 236016, Russia
[2]Innopolis University, Kazan 420500, Russia
[3]Sirius University of Science and Technology, Sochi 354340, Russia
[4]Saratov Branch of Kotel'nikov Institute of Radio Engineering and Electronics of Russian Academy of Sciences, Saratov 410019, Russia
[5]Moscow State University, Moscow 119991, Russia

[a)]**Author to whom correspondence should be addressed:** hramovae@gmail.com

ABSTRACT

We have proposed and studied both numerically and experimentally a multistable system based on a self-sustained Van der Pol oscillator coupled to passive oscillatory circuits. The number of passive oscillators determines the number of multistable oscillatory regimes coexisting in the proposed system. It is shown that our system can be used in robotics applications as a simple model for a central pattern generator (CPG). In this case, the amplitude and phase relations between the active and passive oscillators control a gait, which can be adjusted by changing the system control parameters. Variation of the active oscillator's natural frequency leads to hard switching between the regimes characterized by different phase shifts between the oscillators. In contrast, the external forcing can change the frequency and amplitudes of oscillations, preserving the phase shifts. Therefore, the frequency of the external signal can serve as a control parameter of the model regime and realize a feedback in the proposed CPG depending on the environmental conditions. In particular, it allows one to switch the regime and change the velocity of the robot's gate and tune the gait to the environment. We have also shown that the studied oscillatory regimes in the proposed system are robust and not affected by external noise or fluctuations of the system parameters. Moreover, using the proposed scheme, we simulated the type of bipedal locomotion, including walking and running.

A central pattern generator (CPG) is a biological neural circuit of most vertebrates that controls rhythmic and stereotyped motor behavior (walking, running, swimming, etc.) of practically all vertebrate species by generating rhythmic outputs in the absence of a rhythmic input. The synthetic CPGs made from neuron-like oscillators are used to control artificial objects, for example, walking robots. Currently, there is a great interest in simple and at the same time universal, versatile, and stable CPGs for controlling the movements of robotic systems. Thus, the study of complex nonlinear dynamics of various CPG models is the actual problem nowadays. In this article, we propose a scheme of self-sustained Van der Pol oscillator coupled to a chain of passive oscillatory circuits and investigate its nonlinear dynamics. It is shown that the proposed scheme can serve as an efficient and straightforward CPG for controlling limb movements. We implement the developed CPG model in a physical experiment in the form of an electronic circuit. Finally, we simulate the type of bipedal locomotion by using the proposed scheme, which is promising for robotics applications.

I. INTRODUCTION

Nowadays, the study of limb movement control in robotics attracts much attention. Interest to this problem is caused by the rapid development of technologies and the need for robots both in industry and in everyday life. Particular attention is paid to research aimed at constructing moving mechanical and bionic devices capable of solving complex tasks in changing environmental conditions. In recent decades, the fundamentals of equilibrium-preserving motion have been studied.[1–4] Various methods have been developed, for example, the analytical method, which uses the null-moment point as the primary criterion,[5] the method of controlling the one-leg jumping,[6] and adaptive algorithms,[7,8] among which the method of movement governed by a central pattern generator (CPG)[1,9,10] is one of the closest to the natural movement of living organisms.

It has been shown that a relatively small neural network capable of producing rhythmic processes is responsible for animal's movements.[9,11,12] Such an ensemble of neuron cells is a biological CPG.[13,14] The synthetic CPGs made from neuron-like oscillators are used to control artificial objects.[9] It has been proposed to use a synthetic CPG in the papers,[15,16] in which the models generated the patterns for locomotor activity similar to the living neural networks. The CPG models based on artificial neurons[17–19] usually exploit the principles of machine learning for motion correction.

In robotics, CPGs are often modeled by either spiking neural networks (e.g., based on the FitzHugh–Nagumo models, Hodgkin–Huxley type of neuron models, Matsuoka neural oscillators,[8] or integrate-and-fire neuron models[20,21]) or coupled "classical" nonlinear oscillators (e.g., using Hopf,[22,23] Rayleigh,[24,25] or Van der Pol oscillators[26]). In particular, CPG models have been used with hexapod and octopod robots reproducing insect locomotion.[27] CPGs have also been used for controlling swimming robots, for example, the salamander robot.[28,29] Kimura and coauthors have developed[30] a quadruped walking robot capable of adapting to irregular terrain using a Matsuoka neural oscillator, which is still widely used in CPG models for the gait control.[31] Takeda *et al.*[32] presented a hardware-efficient CPG model implemented in a field programmable gate array to realize a bio-inspired gait of a hexapod robot. Currently, the use of spiking neural networks in the CPG has gained great popularity.[1,33] For example, Lele *et al.* have proposed[34,35] a reinforcement-based stochastic weight update technique to train a spiking CPG for the hexapod robot.

The varying environmental conditions require specific demands to a synthetic CPG: it should tune itself to provide the specific phase shifts of partial oscillators controlling the limb motion.[8,30] Also, the adaptation of CPG natural frequencies to external forcing plays an important role.

The CPGs realized with mathematical models of coupled synchronized nonlinear oscillators are proposed, for example, in papers.[36,37] However, this approach requires high calculation resources and poorly suited for real-time control. Besides, it should be noted that the proposed CPG models usually have a low universality. Consequently, there is currently a significant interest in simple and at the same time universal, versatile, and stable CPGs for controlling the movements of robotic systems.

Thus, the study of complex nonlinear dynamics of various CPG models is very important nowadays[2–4,38] for developing and optimizing CPG systems.[39,40] Moreover, before a proposed CPG model can be applied to a real robotic system, the desired characteristics of that model must be determined and investigated.

In the present paper, we study both experimentally and numerically the nonlinear dynamics and oscillatory regimes in the proposed scheme of the self-sustained Van der Pol (VDP) oscillator coupled to a chain of passive oscillatory circuits. This scheme can be used for the development of CPG controlling the limb movement. We implemented the developed CPG model in a physical experiment in the form of an electronic circuit. Moreover, the type of bipedal locomotion is simulated by using the proposed scheme.

In the well-known papers,[19,26,37,41,42] the networks of VDP oscillators were used as the elements of effective CPGs. However, the network structures of the CPGs considered in these papers have a large number of parameters and are more complex than the CPG scheme proposed in the present paper. Note that we focus here on those features of the nonlinear dynamics of the scheme composed of coupled oscillators that are important for creating an effective and simple CPG.

The paper has the following structure. In Sec. II, we describe the central pattern generator model based on a self-sustained VDP oscillator coupled to a single passive circuit. In Sec. III, we present the results of both the numerical and experimental studies of the CPG based on the VDP oscillator coupled to two passive circuits. In Sec. IV, we study the influence of external noise on the model. In Sec. V, we consider the non-autonomous model with an external harmonic forcing. In Sec. VI, we applied the proposed CPG scheme to generate bipedal gait, including walking and running. In Sec. VII, we discuss and summarize the obtained results.

II. MULTISTABLE SYSTEM WITH ONE ACTIVE AND ONE PASSIVE COUPLED OSCILLATORS

A. Basic scheme and mathematical model

We propose a CPG model based on a simple system of two coupled oscillators where one oscillator is active while another one is a passive linear oscillatory circuit. The corresponding electronic scheme is presented in Fig. 1.

The active oscillator in the system is represented by a softly excited self-sustained oscillator with a cubic nonlinearity and is described by the Van der Pol equation. The passive oscillator is a linear dissipative oscillatory LC-circuit. The soft excitation of the active oscillator is provided by a couple of electronic multipliers (instead of an operational amplifier), which enable the scheme to produce a cubic transformation essential for the classical tube-based VDP oscillator. The multipliers are denoted by $U1$ and $U2$ in Fig. 1(b). The voltage-controlled current source based on the operational amplifier $U3A$ provides excitation of the $L1C2C4$ circuit. The passive oscillator $L2C3$ is coupled to the active one through the coupling capacitor $C1$. The switching of the coexisting regimes can be observed under the variation of the capacity of $C4$, which determines the natural frequency mismatch between the active and passive oscillators.

Let us derive the equations of the scheme shown in Fig. 1(a). The Kirchhoff equations for the currents in the active and passive oscillatory circuits have the following form:

$$\begin{cases} i_{NE} + i_{L_1} + i_{C_{24}} + i_{G_1} + i_{C_1} = 0, \\ i_{C_1} + i_{C_3} + i_{L_2} + i_{G_2} = 0. \end{cases} \tag{1}$$

Here, $i_{C_{24}} = i_{C_2} + i_{C_4}$, and i_{G_1} and i_{G_2} are the currents through resistors in the circuits with the conductances G_1 and G_2, which reflect the total losses in the corresponding circuits. We transform the system (1) into the form with voltages in the circuits,

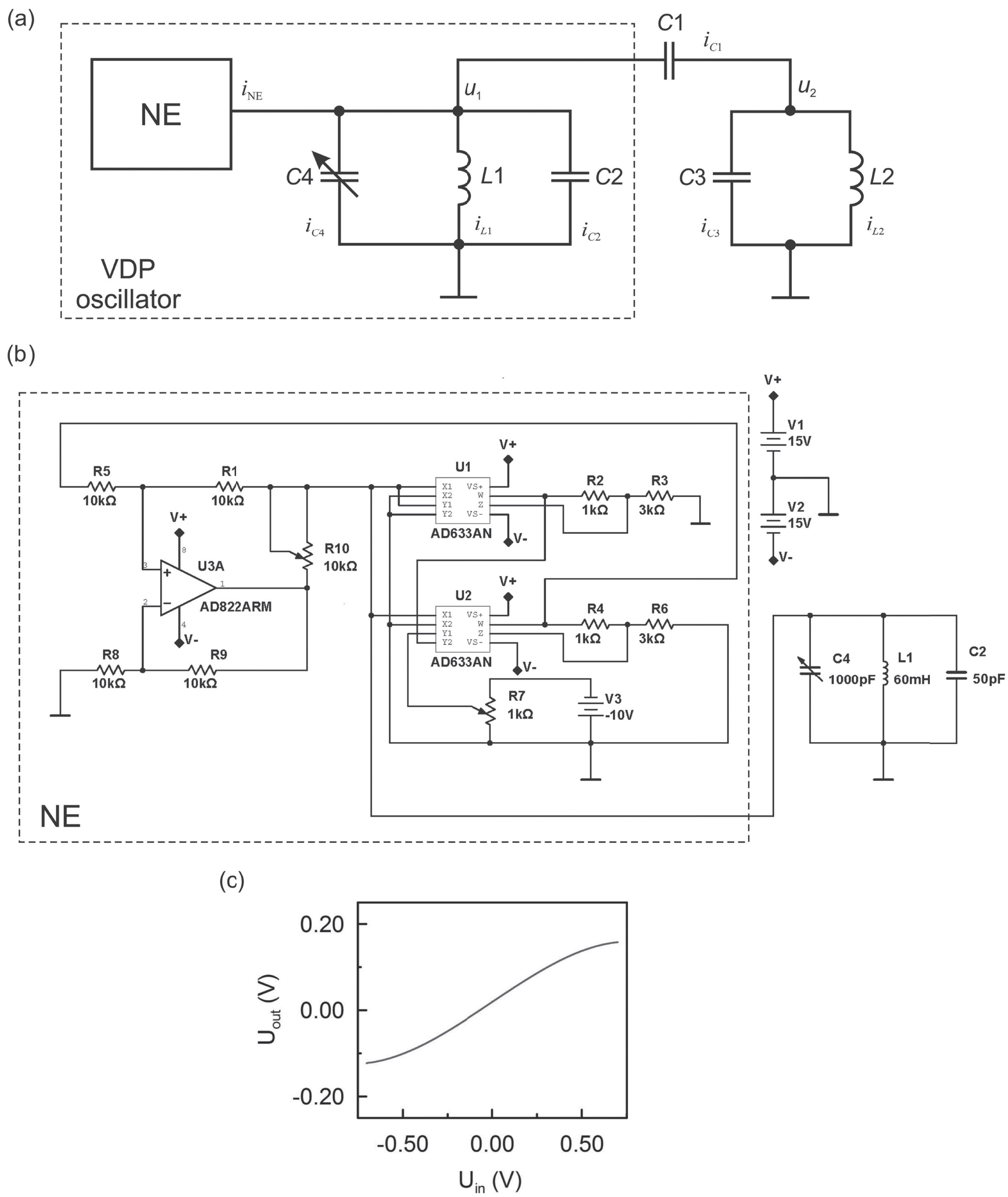

FIG. 1. The scheme of the CPG based on the active VDP oscillator coupled to the passive oscillatory circuit: (a) the general scheme, where "NE" denotes a nonlinear element of Van der Pol oscillator; (b) detailed electronic scheme of the implemented Van der Pol oscillator; (c) the transfer characteristic of the nonlinear element, which is well described by a cubic polynomial function.

taking into account that the volt–ampere characteristic of the nonlinear element [see Fig. 1(c)] is a cubic polynomial function ($i_{NE}(u_1) = -\alpha u_1 + \gamma u_1^3$),

$$\begin{cases} -\alpha u_1 + \gamma u_1^3 + \frac{1}{L_1}\int u_1 dt + C_{24}\frac{du_1}{dt} + G_1 u_1 + C_1 \frac{d(u_1 - u_2)}{dt} = 0, \\ C_1 \frac{d(u_2 - u_1)}{dt} + C_3 \frac{du_2}{dt} + \frac{1}{L_2}\int u_2 dt + G_2 u_2 = 0, \end{cases} \tag{2}$$

where $C_{24} = C_2 + C_4$, and u_1 and u_2 are the voltages in the active and passive circuits, respectively. Differentiating the first and second equations over time and passing to a new dimensionless time $\tau = 1/\sqrt{L_1(C_{24} + C_1)}$, we obtain

$$\begin{cases} \frac{d^2u_1}{d\tau^2} - \sqrt{\frac{L_1}{C_{24}+C_1}}(\alpha - G_1 - 3\gamma u_1^2)\frac{du_1}{d\tau} + u_1 = \frac{C_1}{C_{24}+C_1}\frac{d^2u_2}{d\tau^2}, \\ \frac{d^2u_2}{d\tau^2} + \frac{G_2\sqrt{L_1(C_{24}+C_1)}}{C_1+C_3}\frac{du_2}{d\tau} + \frac{L_1(C_{24}+C_1)}{L_2(C_1+C_3)}u_2 = \frac{C_1}{C_1+C_3}\frac{d^2u_1}{d\tau^2}. \end{cases} \tag{3}$$

Then, replacing the variables and parameters as follows:

$$\begin{cases} x_i = \frac{u_i}{u_0}\sqrt{3\gamma\sqrt{\frac{L_1}{C_{24}+C_1}}}, \quad u_0 = 1\,V, \quad \varepsilon = \sqrt{\frac{L_1}{C_{24}+C_1}}(\alpha - G_1), \\ \gamma_{12} = \frac{C_1}{C_{24}+C_1}, \quad \gamma_{21} = \frac{C_1}{C_1+C_3}, \quad 2\beta_1 = \frac{G_2\sqrt{L_1(C_{24}+C_1)}}{C_1+C_3}, \\ p_1^2 = \frac{L_1(C_{24}+C_1)}{L_2(C_1+C_3)}, \end{cases} \tag{4}$$

we obtain equations in the form of two coupled oscillators, which describe the dynamics of the considered system (Fig. 1),

$$\begin{cases} \ddot{x}_1 - (\varepsilon - {x_1}^2)\dot{x}_1 + x_1 = \gamma_{12}\ddot{x}_2, \\ \ddot{x}_2 + 2\beta_1\dot{x}_2 + {p_1}^2 x_2 = \gamma_{21}\ddot{x}_1. \end{cases} \tag{5}$$

Here, ε is the dissipation parameter controlling the energy pumping of the active oscillator, β_1 is the dissipation parameter of the passive oscillator, p_1 is the parameter determining the natural frequency mismatch between the oscillators, and γ_{12} and γ_{21} are the coupling parameters between the corresponding oscillators. Thus, the system (5) is considered as a mathematical model for the central pattern generator consisting of the active VDP oscillator and the passive linear LC-oscillator.

B. Experimental analysis

The bifurcation analysis carried out in Ref. 43 shows that the phase space of the considered coupled active and passive oscillators contains two stable limit cycles for specific values of the coupling coefficients between the oscillators in (5). Hence, the introduction of the correct mismatch of the natural frequencies of the passive and active oscillators allows one to obtain the coexistence of two self-sustained multistable oscillatory regimes with different phase relations. Since the stable limit cycles have different frequencies, we can expect that the frequency locking of each oscillatory regime will appear at different frequencies of the external forcing.

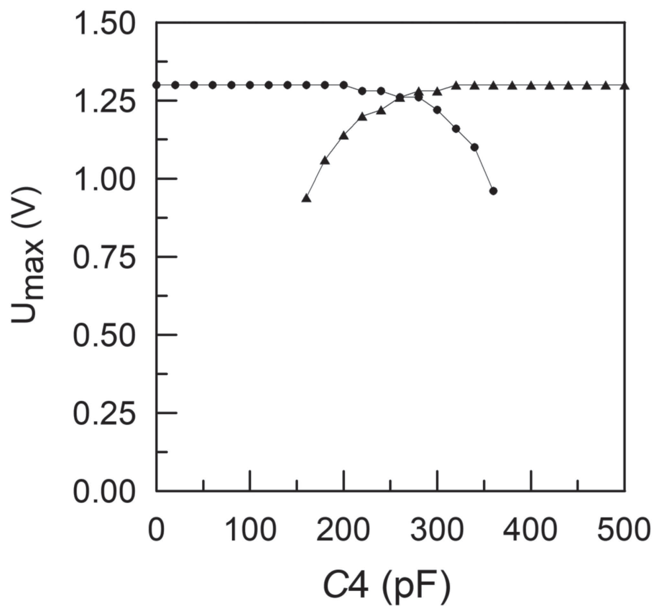

FIG. 2. The amplitude of voltage oscillations in the active self-sustained oscillator of the coupled system (see Fig. 1) vs the value of $C4$ capacitance.

To develop the controlling approach, we carried out an experiment that shows the dependence of the amplitude $U_{\max}$ of oscillations in the active circuit on the control parameter $C4$. $U_{\max}$ was measured from the point u_1 in Fig. 1(a). The experimental results are presented in Fig. 2, where the circles denote the amplitude values at $C4$ increasing, and triangles denote the amplitudes at $C4$ decreasing. One can see that the increase in the capacitance up to $C4 = 350$ pF leads to the smooth decrease in the amplitude. With a further increase in $C4$, a hard transition to the oscillations with a larger amplitude is observed at $C4 = 350$ pF. The backward changing of the parameter $C4$ forces the system to return to the initial regime at $C4 = 150$ pF.

Figure 3 represents the experimental time series and phase portraits of the higher-amplitude signal corresponding to the voltage in the active VDP oscillator and the lower-amplitude oscillations corresponding to the passive oscillatory circuit. For generality, the time t in Fig. 3 is normalized to the period of oscillations in the passive circuit: $t_0 = t/(2\pi\sqrt{L_2C_3})$. Figures 3(a) and 3(b) show the time series and phase portrait before the bifurcation transition. In this regime, the signals are in-phase. Figures 3(c) and 3(d) depict the time series and phase portrait after the bifurcation transition. In this case, the shift between the signals is equal to the half of the characteristic period of oscillations. The phase shift depends on the value of $C4$ capacitance.

Hence, the system allows one to switch the phase shifts between the oscillations in the subsystems by smooth variation of the frequency mismatch parameter. Moreover, in this case, we observe the hysteresis in the occurrence of in-phase and anti-phase oscillations.

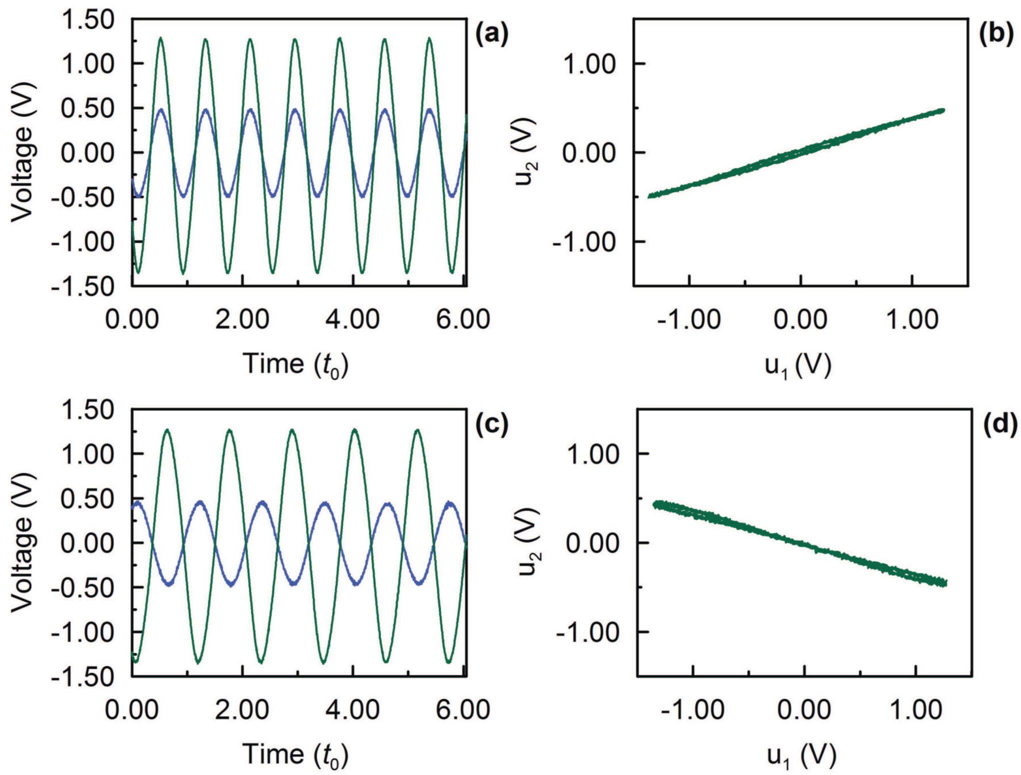

FIG. 3. Experimental time series [(a) and (c)] and corresponding phase portraits [(b) and (d)] of the system with one active (VDP) and one passive oscillators before [(a) and (b)] and after [(c) and (d)] the bifurcation transition; $C4 = 200$ pF [(a) and (b)] and $C4 = 400$ pF [(c) and (d)]. Green curve in time series corresponds to the signal u_1 from the VDP oscillator [see Fig. 1(a)] and blue curve corresponds to the signal u_2 from the passive oscillatory circuit.

III. MULTISTABLE SYSTEM WITH ONE ACTIVE AND TWO PASSIVE COUPLED OSCILLATORS

The system considered in Sec. II is the simplest model of a multi-mode self-sustained oscillator. In Sec. III, we study the more complex case of the system with one active (VDP) and two passive oscillators capable of generating signals with multiple independent time scales. This feature is essential for the development of effective CPG models.

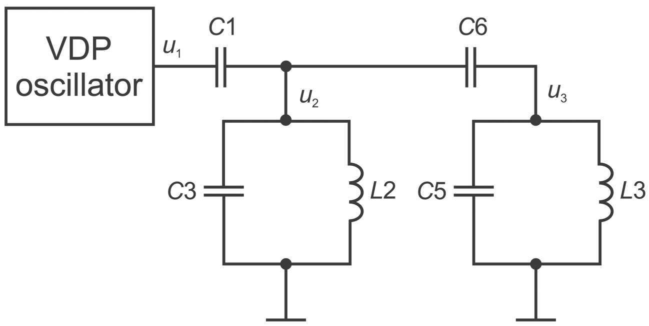

FIG. 4. The scheme of the CPG based on the active VDP oscillator coupled with two passive oscillators. Here, $C5 = C3$, $L3 = L2$, and $C6 = C1$.

We have added to the system a passive circuit composed of $L3C5$ components. A simplified scheme of the model consisting of an active oscillator and a chain of passive oscillators is presented in Fig. 4. The values of the elements in the second passive oscillator and the coupling capacitor are the same as in the scheme with a single passive circuit (see Fig. 1).

The Kirchhoff equations for the considered scheme have the following form:

$$\begin{cases} -\alpha u_1 + \gamma u_1^3 + \dfrac{1}{L_1}\displaystyle\int u_1 dt + C_{24}\dfrac{du_1}{dt} + G_1 u_1 + C_1\dfrac{d(u_1 - u_2)}{dt} = 0, \\ C_1\dfrac{d(u_2 - u_1)}{dt} + C_3\dfrac{du_2}{dt} + \dfrac{1}{L_2}\displaystyle\int u_2 dt + G_2 u_2 + C_6\dfrac{d(u_2 - u_3)}{dt} = 0, \\ C_6\dfrac{d(u_3 - u_2)}{dt} + C_5\dfrac{du_3}{dt} + \dfrac{1}{L_3}\displaystyle\int u_3 dt + G_3 u_3 = 0. \end{cases} \tag{6}$$

Here, the designations are similar to those used in Eq. (2). G_3 is the conductance of the resistor in the second passive circuit, which reflects the total losses in the circuit and u_3 is the voltage in the second circuit. Performing transformations similar to those in Sec. II A, we obtain the following equations in the normalized variables, which describe the dynamics of the system:

$$\begin{cases} \ddot{x}_1 - \left(\varepsilon - x_1^2\right)\dot{x}_1 + x_1 = \gamma_{12}\ddot{x}_2, \\ \ddot{x}_2 + 2\beta_1\dot{x}_2 + p_1^2 x_2 = \gamma_{21}\ddot{x}_1 + \gamma_{23}\ddot{x}_3, \\ \ddot{x}_3 + 2\beta_2\dot{x}_3 + p_2^2 x_3 = \gamma_{32}\ddot{x}_2, \end{cases} \tag{7}$$

where

$$\begin{aligned} \gamma_{12} &= \frac{C_1}{C_{24}+C_1}, \quad \gamma_{21} = \frac{C_{24}}{C_1+C_3+C_6}, \\ \gamma_{23} &= \frac{C_6}{C_1+C_3+C_6}, \quad \gamma_{32} = \frac{C_6}{C_5+C_6}, \\ 2\beta_1 &= \frac{G_2\sqrt{L_1(C_{24}+C_1)}}{C_1+C_3+C_6}, \quad 2\beta_2 = \frac{G_3\sqrt{L_1(C_{24}+C_1)}}{C_5+C_6}, \\ p_1^2 &= \frac{L_1(C_{24}+C_1)}{L_2(C_1+C_3+C_6)}, \quad p_2^2 = \frac{L_1(C_{24}+C_1)}{L_3(C_5+C_6)}. \end{aligned} \tag{8}$$

Here, $\beta_{1,2}$ are the dissipation parameters of the passive oscillators, $p_{1,2}$ are the parameters determining the natural frequency mismatch between the active and corresponding passive oscillators, $\gamma_{12,21,23,32}$ are the coupling parameters between the corresponding oscillators, and ε and x_i are determined as in (4). Thus, the system (7) can be considered as a mathematical model of the CPG consisting of Van der Pol oscillator and two passive linear LC-oscillators. We used the XPPAUT software[44] to carry out the bifurcation analysis.

The considered model exhibits a self-oscillatory regime represented by a limit cycle and possesses bistability and hysteresis. The bifurcations underlying the observed bistability are represented in the numerically obtained bifurcation diagram in Fig. 5. One can see that the subcritical Neimark–Sacker bifurcation underlies the

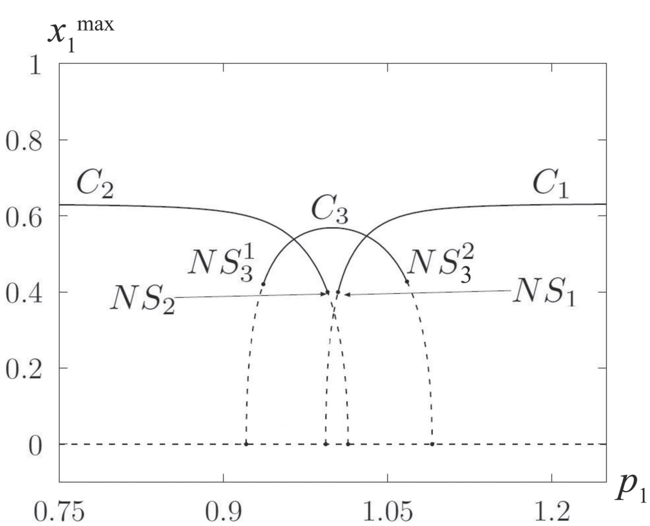

FIG. 5. Characteristic bifurcation diagram for the model (7) with two passive coupled oscillators. Here, $C_{1,2,3}$ are the limit cycles, $NS_{1,2}$ and $NS_3^{1,2}$ are the bifurcation points for Neimark–Sacker bifurcation. The dashed lines represent unstable limit sets, while the solid lines represent stable limit cycles.

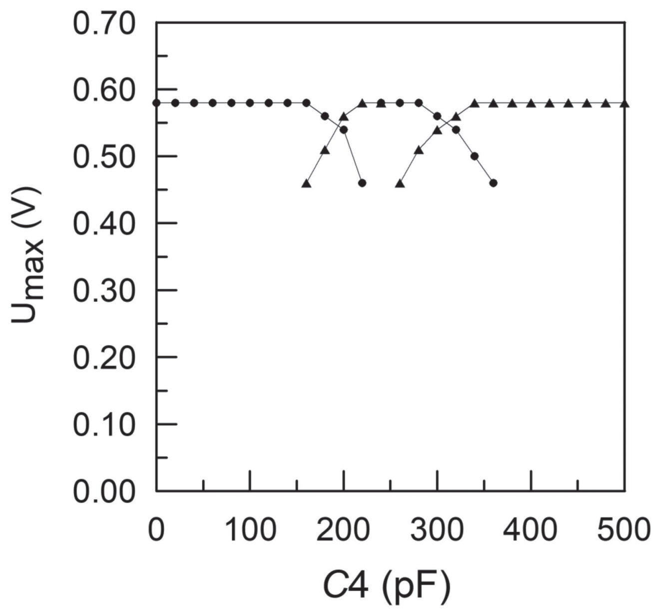

FIG. 6. The amplitude of voltage oscillations in the active oscillator of the system (see Fig. 4) vs the value of $C4$ capacitance.

occurrence of coexisting stable limit cycles in the phase space of the dynamical system. This bifurcation mechanism was studied in detail[43] for the VDP oscillator system coupled with one linear dissipative oscillatory circuit. One should note that different phase shifts between dynamical variables characterize the coexisting self-oscillatory regimes, and their occurrence and collapse take place with an increase or decrease in the control parameter p_1. We will show further that such properties can be effectively used for the CPG development.

We have experimentally studied the scheme in Fig. 4 and obtained the dependence of the amplitude of voltage oscillations on the control parameter $C4$. The voltage amplitude U_{max} is presented vs the value of $C4$ in Fig. 6. Here, the dependence of the amplitude on the increasing and decreasing $C4$ is denoted with circles and triangles, respectively. With the increase in $C4$, U_{max} shows at first a smooth decrease and then hardly switches at $C4 = 220$ pF to a higher value due to Neimark–Sacker bifurcation. The second hard transition is observed at $C4 = 380$ pF. The backward movement along the $C4$ axis leads to hard backward transitions at $C4 = 250$ pF and $C4 = 150$ pF, respectively. Thus, the experimentally obtained results are consistent with the results of numerical simulation.

Figure 7 represents the experimental time series and phase portraits of the regimes observed in the system. Figures 7(a) and 7(b) correspond to the regime before all bifurcation transitions when all signals are in-phase. Figures 7(c) and 7(d) demonstrate the signals and phase portraits after the first bifurcation transition. In this regime, VDP oscillator is in-phase with the first passive oscillator and anti-phase with the second one. Figures 7(e) and 7(f) show the time series and phase portraits after the second bifurcation transition. In this case, the active and the second passive oscillators are

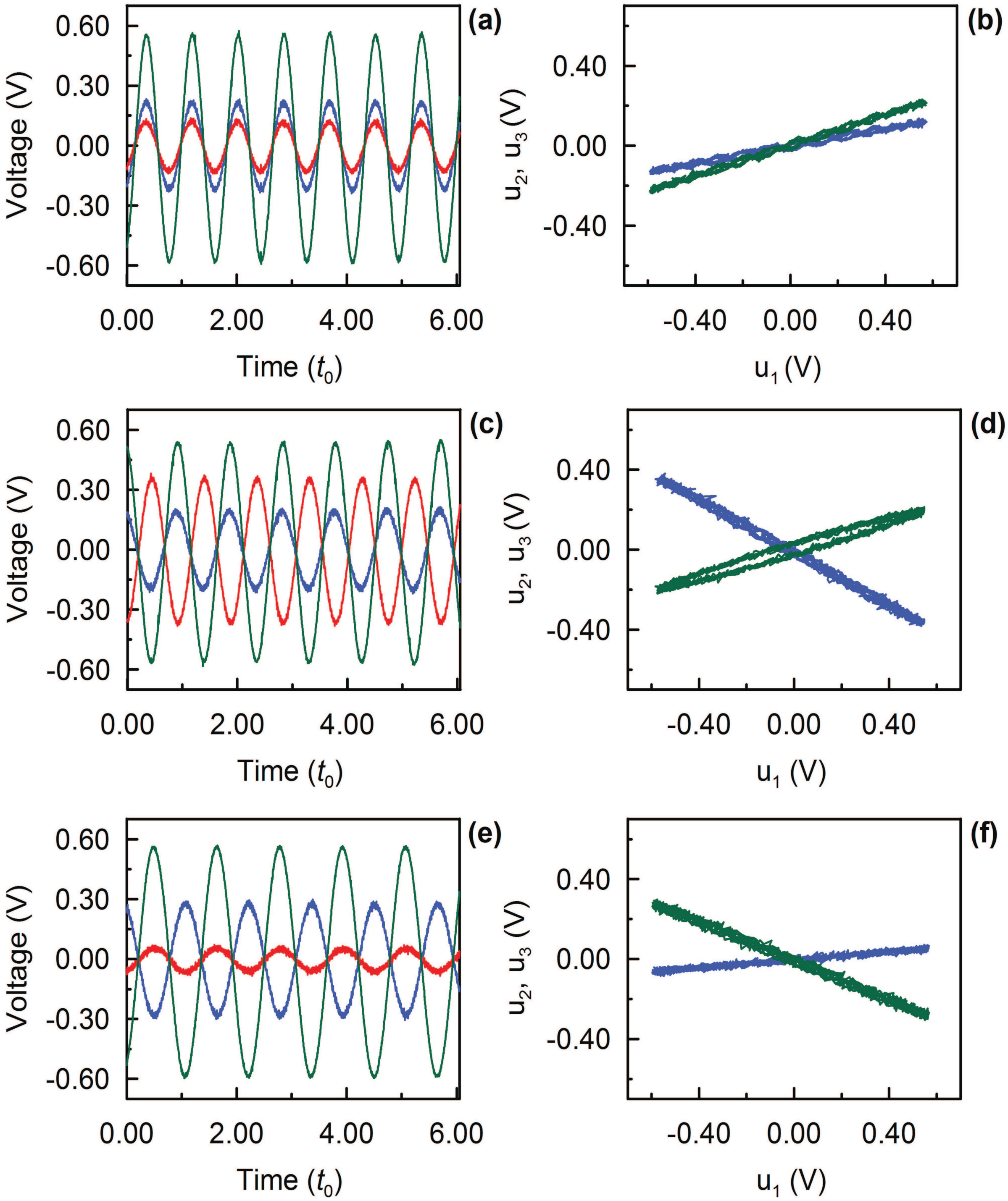

FIG. 7. Experimental time series and phase portraits of the system with one active (VDP) and two passive oscillators before [(a) and (b)], after the first (c) and (d), and after the second [(e) and (f)] bifurcation transition; $C4 = 150$ pF [(a) and (b)], $C4 = 250$ pF [(c) and (d)], and $C4 = 400$ pF [(e) and (f)]. Green curve in the time series corresponds to the signal u_1 from the VDP oscillator (see Fig. 4), blue curve corresponds to the signal u_2 from the first passive oscillatory circuit, and red curve corresponds to the signal u_3 from the second passive oscillatory circuit.

in-phase, while the first passive oscillator is anti-phase with respect to them. Moreover, the ratio of signal amplitudes changes after the bifurcations.

We assume that the observed hard transitions point to the coexistence of three stable oscillatory regimes characterized by different phase shifts between the oscillations in the active and passive oscillators of the system. These regimes are robust as the variation of the system parameters does not lead to qualitative changes in their behavior.

Therefore, the studied model is supposed to be useful as a CPG for a walking robot.

IV. INFLUENCE OF NOISE

Considering that the real environment is commonly exposed to noises of various nature, CPG is necessary to be stable in the presence of noises. In the experiment, we have studied the influence of noise on switching between the coexisting oscillatory regimes in the system with two passive circuits.

We applied white Gaussian noise from the function generator 81150A Agilent Technologies (denoted by "GS") to the system's active oscillator using the capacitive coupling (see Fig. 8). Two cases were considered: (i) the noise amplitude is four times smaller than the amplitude of the voltage in the active oscillator, i.e., the signal-to-noise ratio (SNR) was 24 dB; (ii) SNR = 12 dB. Note that the introduced noise does not affect the mean frequency of oscillations in the system.

In Fig. 9, we present the experimental time series. Comparison of Figs. 7(c) and 9 shows that the switching of oscillatory regimes is realized even when SNR = 12 dB, and the phase shifts between the signals are maintained even at high levels of noise. Hence, the proposed CPG model remains stable in the presence of intensive noise that is very important for robotics applications.

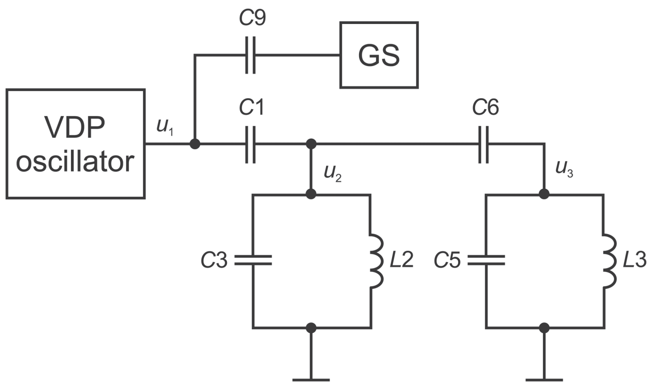

FIG. 8. The scheme of the CPG in the presence of noise or external forcing; $C9 = C1$.

V. CPG DYNAMICS UNDER EXTERNAL FORCING

In this section, we study the ability of the proposed CPG model to adjust to changes in the environmental conditions by changing the frequency and phase relations of the coupled oscillators. To model the CPG behavior under an external influence, we introduced an external harmonic forcing $A\cos(ft)$ to the active VDP oscillator of the system having two passive circuits (see Fig. 8),

$$\begin{cases} \ddot{x}_1 - \left(\varepsilon - x_1^2\right)\dot{x}_1 + x_1 = \gamma_{12}\ddot{x}_2 + A\cos ft, \\ \ddot{x}_2 + 2\beta_1\dot{x}_2 + p_1^2 x_2 = \gamma_{21}\ddot{x}_1 + \gamma_{23}\ddot{x}_3, \\ \ddot{x}_3 + 2\beta_2\dot{x}_3 + p_2^2 x_3 = \gamma_{32}\ddot{x}_2. \end{cases} \tag{9}$$

The synchronization phenomenon explains the dynamics of the proposed system under external forcing (e.g., see Ref. 45, in

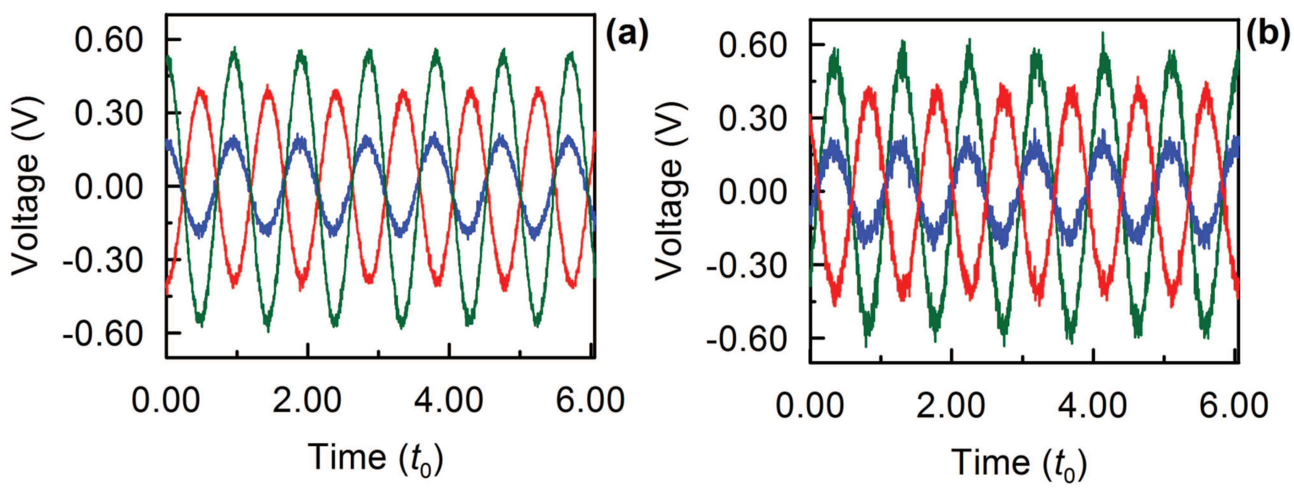

FIG. 9. Experimental time series of the system with one active and two passive oscillators ($C4 = 250$ pF) for the following values of the external noise intensities: (a) SNR = 24 dB and (b) SNR = 12 dB. Green curve in the time series corresponds to the signal u_1 from the VDP oscillator (see Fig. 8), blue curve corresponds to the signal u_2 from the first passive oscillatory circuit, and red curve corresponds to the signal u_3 from the second passive oscillatory circuit.

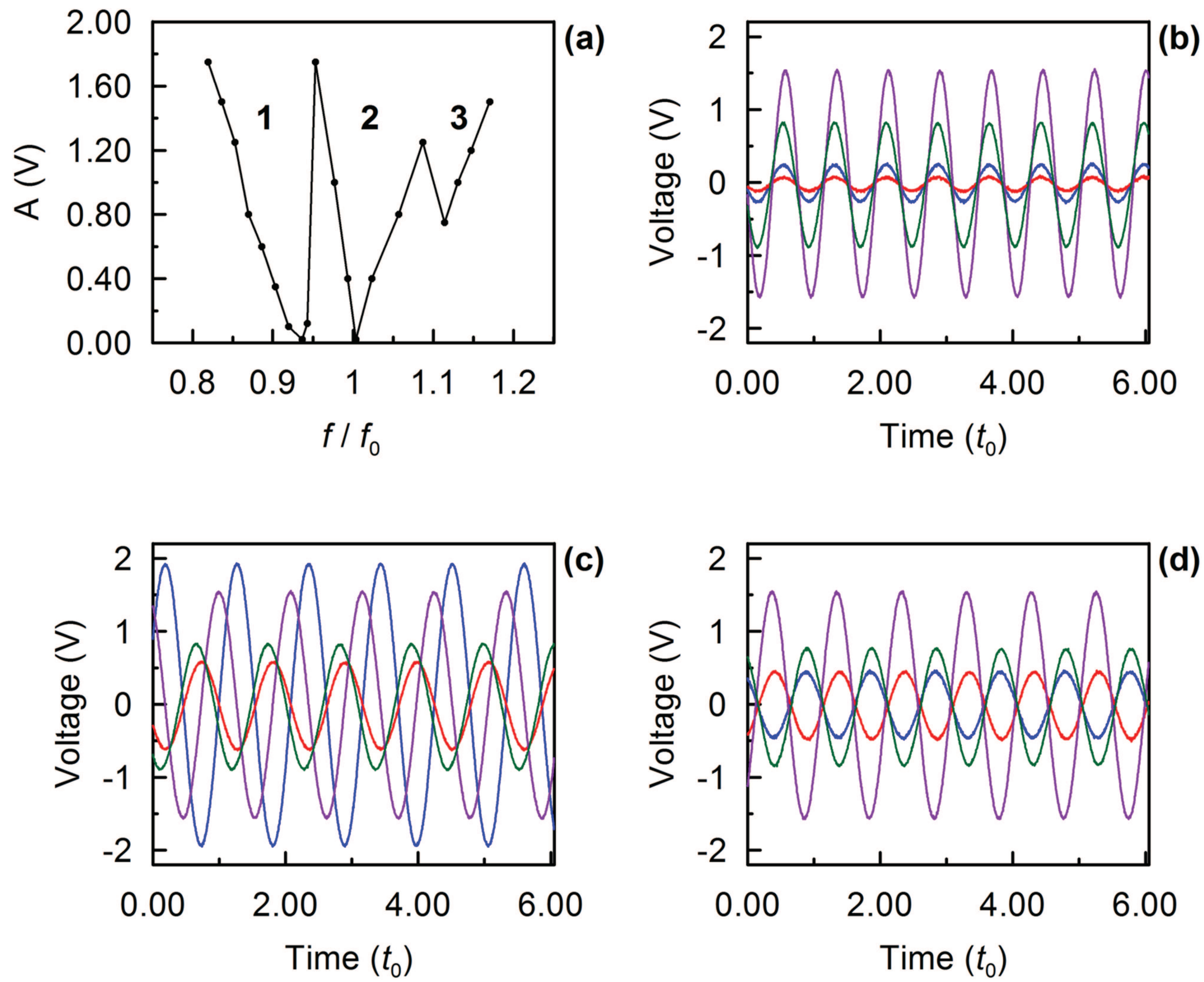

FIG. 10. (a) The chart of regimes of the CPG model under external harmonic forcing; $C4 = 170$ pF. Experimental time series of the system for regime 3 ($f/f_0 = 1.13$) on the chart (b), regime 1 ($f/f_0 = 0.93$) (c), and regime 2 ($f/f_0 = 1$) (d); $A = 1.5$ V. Green curve in the time series corresponds to the signal u_1 from the VDP oscillator (see Fig. 8), blue curve corresponds to the signal u_2 from the first passive oscillatory circuit, red curve corresponds to the signal u_3 from the second passive oscillatory circuit, and purple curve corresponds to the signal of the external harmonic forcing.

which a detailed theoretical study of the influence of external harmonic forcing on the dynamics of coupled Van der Pol oscillators was carried out). In Fig. 10, we show the results of the experiment at $C4 = 170$ pF. Varying the amplitude and the frequency of external forcing, we obtained the boundaries of the region where the system exhibits periodic oscillations. Outside this region, the system demonstrates two-frequency quasi-periodic dynamics. Figure 10 shows that by changing the external forcing frequency, it is possible to obtain three synchronization regions corresponding to different oscillatory regimes. The frequency of the external forcing f is normalized in Fig. 10 to the resonant frequency f_0 of the first passive circuit. In the third synchronization tongue with the bottom at $f/f_0 \approx 1.13$ and $A \approx 0.8$ V, we observe the regime [Fig. 10(b)], in which all three oscillators are synchronous. In the second synchronization tongue ($f/f_0 \approx 1$), the system switches to the dynamics [see Fig. 10(d)] similar to the regime in Fig. 7(c). In this regime, the VDP oscillator is in-phase with the first passive oscillator and anti-phase with the second one. Finally, the system undergoes the second bifurcation near $f/f_0 \approx 0.93$ [Fig. 10(c)] and demonstrates in the first synchronization tongue the dynamics similar to the regime of the autonomous system shown in Fig. 7(e). In this case, the active and the second passive oscillators are in-phase, while the first passive oscillator is anti-phase with respect to them. Hence, for controlling the types of movement, one can change the value of the active

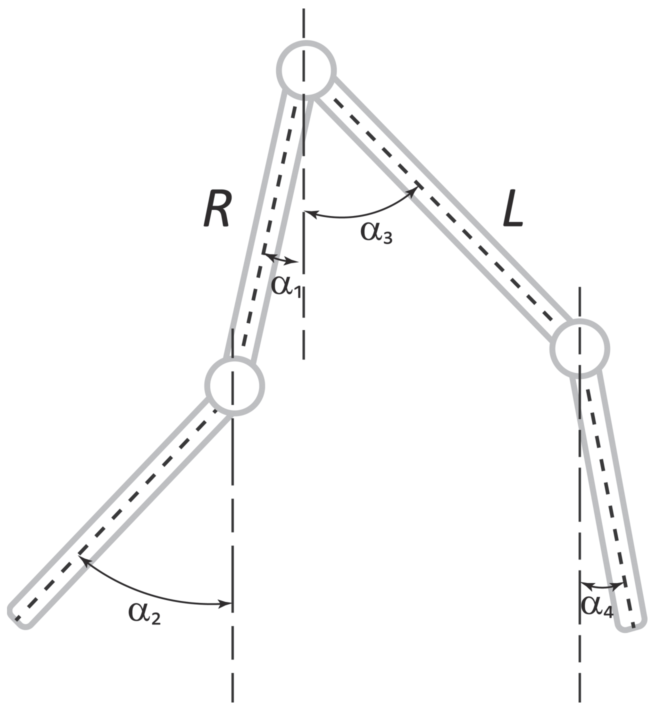

FIG. 11. Biped model with two joints per leg; "R" denotes the right leg and "L" denotes the left leg. All angles are measured positively clockwise from vertical.

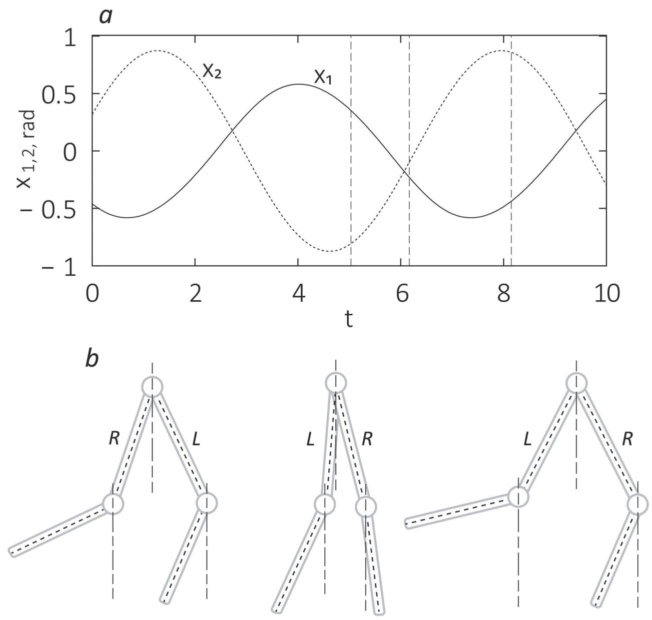

FIG. 12. (a) Time series generated by the CPG, which define the angular displacements for the thigh and shin of the first leg in the regime of running; x_1 is the signal from the VDP oscillator (see Fig. 4), x_2 is the signal from the first passive circuit; $\tau = \pi$, $A = 0.03$, and $f = 0.94$. (b) Snapshots of simulated biped running gait at the time moments denoted by vertical dashed lines in (a).

element $C4$ in the ensemble and change the frequency of external forcing.

Thus, varying the frequency of the external forcing, one can lock the frequency of the CPG and control the frequency of oscillations in the CPG, the ratio of signal amplitudes, and phase shifts between oscillators corresponding to coexisting stable limit cycles.

VI. CPG SCHEME IMPLEMENTATION

We applied the proposed CPG scheme for the biped model for generating the rhythm providing walking/running regimes. For this purpose, the scheme with two passive circuits (see Fig. 4) is the most appropriate. Figure 11 represents a simplified biped model with two joints per leg. Each joint of the right leg moves with angular displacements determined by the scheme's outputs x_1 and x_2 in the following way: $\alpha_1 = x_1$ and $\alpha_2 = x_1 + |x_2|$. Such a definition of α_2 prevents the physiologically impossible turns of the knee joint. The angular displacements of the left leg are determined similarly but with a delay of τ relative to the right leg. Note that the value of τ affects the type of gait.

Let us consider the scenario of the CPG scheme operation demonstrating the possibility of switching the gait type. Suppose that the biped object runs in a straight line on a flat surface, and it has to change the type of gait from running to walking at a certain point P. Moreover, the switching from running to walking must occur smoothly. Such a scenario may occur, for example, if the type of surface changes at point P.

The CPG scheme parameters were chosen based on the results of the carried out analysis (see Secs. II–V). The CPG scheme with two passive circuits under external harmonic forcing with dimensionless amplitude A and frequency f implements the necessary sequence of gait types. Figure 12 illustrates the regime of running gait when $A = 0.03$ and $f = 0.94$. In this case, the higher amplitude signal [the dotted curve in Fig. 12(a)] controls the rotation angle of the shin, while the lower amplitude signal (the solid curve) controls the rotation angle of the thigh. The selected ratio of the signal amplitudes and the phase shift between the signals provide the gait similar to human running.[46,47] The simulated movement of the biped model is graphically displayed at several time moments to verify the results qualitatively [see Fig. 12(b)].

Suppose that the biped object "detects" the point P at distance L from it and begins to slow down smoothly. This regime can be implemented by changing the frequency of external forcing in the CPG scheme by the following expression: $f = 0.94 + 0.006 \times (1 - l/L)$, where l is the current distance to the point P. This leads to a smooth decrease in the amplitudes of the control signals, a change in the phase shift between them, and, as a result, to a slowdown in the running speed. Figure 13 shows this regime when $l/L = 0.5$.

Finally, the gait type of the biped object switches to walking at point P by switching off the external forcing ($A = 0$), leading to the change in the ratio of amplitudes of the control signals (see Fig. 14). This is a consequence of the change in the CPG oscillatory regime. In this case, the amplitude of the shin's swing becomes less than that

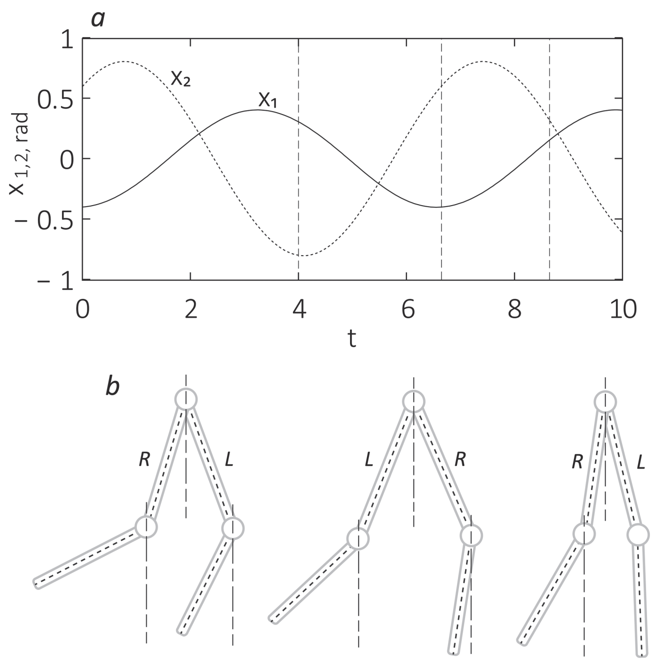

FIG. 13. (a) Time series generated by the CPG, which define the angular displacements for the thigh and shin of the first leg in the regime of running that is slower than running regime in Fig. 12; $\tau = \pi$, $A = 0.03$, and $f = 0.943$. (b) Snapshots of simulated biped slow running gait at the time moments denoted by vertical dashed lines in (a).

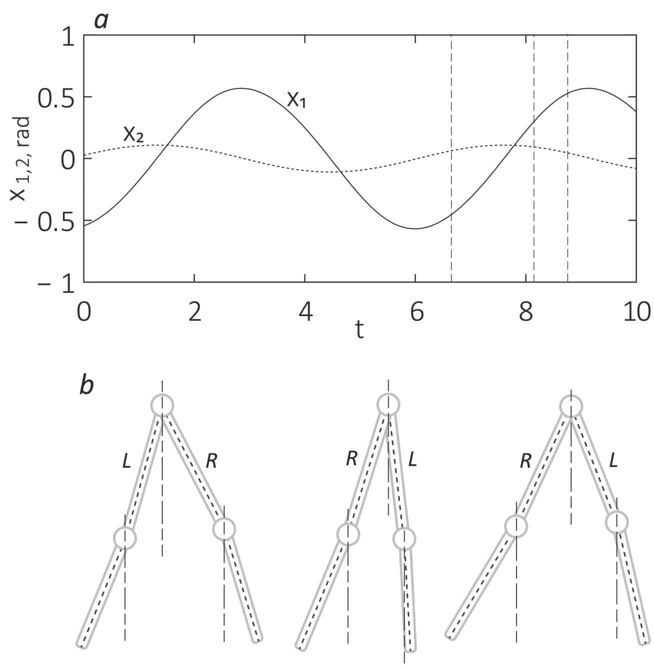

FIG. 14. (a) Time series generated by the CPG, which define the angular displacements for the thigh and shin of the first leg in the regime of walking; $\tau = \pi$ and $A = 0$. (b) Snapshots of simulated biped walking gait at the time moments denoted by vertical dashed lines in (a).

for the thigh. Figure 14(b) shows schematically the generated gait that is qualitatively similar to human walking.[46,47]

VII. DISCUSSION AND CONCLUSIONS

The considered biped model exhibits coordinated motions quite similar to human walking and running. Thus, in this article, the proposed CPG scheme has proven to be useful for the generation of trajectory patterns for rhythmic locomotion. We should note that the study is strictly a kinematic example.

Van der Pol oscillators were already considered as the elements of CPG for various walking machines in several earlier articles. In particular, Bay *et al.*[37] have modeled CPG by the network of coupled VDP oscillators and demonstrated its application for a simple biped locomotory system. Similar to the latter study, but more comprehensive analysis was conducted by Dutra *et al.*[42] Moreover, Zielinska[41] compared the gait generated by four coupled VDP oscillators with the natural human gait and showed good conformity between them. Liu *et al.* have shown[26] that the CPG network formed by a set of mutually coupled mathematical models of VDP oscillators is effective for generating the rhythmic movement patterns for multi-joint robots. Yu *et al.* have developed a two-layered CPG-based controller for generating the rhythmic movement for legs of the hexapod walking robot with the VDP oscillator employed on the high layer.[19] Bahramian *et al.*[48] proposed a new nonlinear coupling between VDP oscillators in the network that improves the CPG performance.

The principal difference of the present work is the implementation of the proposed CPG in the form of a radio engineering circuit and not in the form of a mathematical model, as was done in the other works. The proposed CPG is more straightforward because it consists of just one active VDP oscillator coupled to several passive circuits. Moreover, we considered the non-autonomous scheme with external forcing to verify the possibility of the additional control of CPG.

We have shown that the proposed CPG scheme enables switching between different types of locomotion. We have obtained the experimental results demonstrating the presence of multistability, i.e., the coexistence of oscillatory regimes in the considered system of coupled oscillators. It is found out that, depending on the number of passive oscillators, there can coexist two or three stable oscillatory regimes in the system. The amplitude and phase relations between the active and passive oscillators control the gait, which features can be adjusted depending on the external conditions. Variation of the active oscillator's natural frequency leads to hard switching between the oscillatory regimes in the system.

In the system with two additional passive circuits, all oscillators remain in-phase, having different amplitudes in the first regime. In the second and the third regimes, one of the passive oscillators is in-phase to the active VDP oscillator, while another passive oscillator is anti-phase to it.

We have also studied the structure of the parameter space for the non-autonomous system and the properties of switching between the oscillatory regimes. We have found out that there are two synchronization regions in the system corresponding to different oscillatory regimes. The external harmonic forcing allows one to control the switching between the regimes. Therefore, the external signal frequency can serve as a parameter to control the types of behavior of the model and realize a feedback in the proposed CPG. The possibility of implementing the feedback in the CPG scheme is important because it will allow one to change the characteristics of the patterns formed by the CPG and the movements controlled by them, depending on the environmental conditions. For example, a signal from a sensor measuring the distance to an obstacle or a command generated by processing an image from an artificial vision system can be used as a control signal for implementing the feedback. The carried out analysis has also shown that the studied oscillatory regimes are robust and not affected by external noise or fluctuations of the system parameters.

During the transition from a regime with one phase shift to a regime with another phase shift, the transient process can take quite a long time. First of all, this is due to the high Q-factors of additional oscillatory circuits connected to the Van der Pol generator. Nevertheless, the transition time significantly decreases with decreasing the Q-factor of the additional circuit. For example, if the inductor's internal resistance is 100 Ω, the time to establish the phase difference during the transition from the in-phase regime to the anti-phase regime and back is about two characteristic oscillation periods. Thus, we avoid the difficulties associated with the influence of transient processes on locomotion. Remarkably, living organisms also require a finite time to switch from one type of gait to another,[49,50] and the proposed CPG system models approximately this behavior.

Moreover, planning a strategy for using the CPG, one has to take into account the presence of hysteresis in the system. For example, suppose one plan to control the gait type by changing the main control parameter in the autonomous CPG. In this case, one can avoid hysteresis due to an abrupt change in the control parameter and, consequently, jumping over the hysteresis region. On the other hand, the hysteresis effect can be valuable in modeling the behavior similar to the behavior of living organisms because the transition between gait regimes in animals usually occurs with hysteresis[49,50].

Finally, we discuss the advantages of the proposed CPG scheme based on Van der Pol oscillator, namely,

- Ease of implementation from a technical standpoint.
- Ease of setting parameters due to the system's deterministic nature; there is no need for prior training of the system. We should note that the parameters are usually tuned by the trial-and-error method or by an optimization algorithm.[51]
- The stability of the output control signals and the simplicity of tuning their characteristics. For example, the generation regime depends only on the circuit parameters and the external signal (if any).
- Scalability and versatility: The ability to create an ensemble of *N* coupled oscillators, where each element of the ensemble controls the movement of an individual limb or individual joint, while the fixed phase difference between the output control signals and the ratio of their amplitudes are determined by the parameters of the ensemble elements and the external signal (if any). This allows one to control the gait characteristics (walking/running, speed, etc.) by adjusting the parameters of the ensemble elements, including the case of a multi-legged robotic system.
- The influence of the external signal on the oscillation characteristics of individual circuits in the ensemble (their frequency, amplitudes, and phase shifts between them) allows one to implement a sensory feedback in the CPG based on such an ensemble of oscillators where the signal generated in accordance with the environmental data acts as an external control signal.
- Using such systems for the generation of control policies reduces the dimensionality of the control problem that helps to deal with robots with multi-DOFs.[26]

Finally, we have proposed the simple CPG model, which can be used in a broad spectrum of robotics applications. In particular, it allows one to switch the regime and change the velocity of the bipedal robot's gate and tune the gait to the environment. As a basis for the CPG, we chose and studied a multi-stable self-oscillating system—the Van der Pol oscillator—where the control parameter variation can change the phase shifts between the oscillations in subsystems (i.e., partial oscillators) and the ratio of the oscillation amplitudes. In contrast, the external forcing can change the frequency and amplitudes of oscillations, preserving the phase shifts. The physical experiments and the example of the CPG implementation for the biped model completely confirm the efficiency of the proposed scheme.

ACKNOWLEDGMENTS

This study was supported by the Ministry of Science and Higher Education of the Russian Federation (Agreement No. 075-02-2021-1748). D.D.K., V.I.P., M.D.P., and A.E.H. carried out this work within the framework of the state task of SB IRE RAS. A.E.H. received support from Scientific School Support Grant No. NSH-589.2022.1.2 in formulating research objectives. The authors acknowledge Elena Pitsik for assistance in the preparation of illustrative materials.

AUTHOR DECLARATIONS

Conflict of Interest

The authors have no conflicts to disclose.

DATA AVAILABILITY

The data that support the findings of this study are available within the article.

REFERENCES

[1] L. M. Izquierdo-Córdoba, J. M. Rosário, and D. A. Hurtado, "Hybrid dynamic modelling and bioinspired control based on central pattern generator of biped robotic gait," in *Advanced Robotics and Intelligent Automation in Manufacturing* (IGI Global, 2020), pp. 233–268.
[2] S. Aoi and K. Tsuchiya, "Self-stability of a simple walking model driven by a rhythmic signal," Nonlinear Dyn. **48**, 1–16 (2007).
[3] A. Zelei, B. Krauskopf, P. T. Piiroinen, and T. Insperger, "Stable periodic motion of a controlled segmented leg model of pedal locomotion with inelastic ground-foot collision," Nonlinear Dyn. **97**, 1945–1958 (2019).

[4]C. M. Pinto, "Stability of quadruped robots' trajectories subjected to discrete perturbations," Nonlinear Dyn. **70**, 2089–2094 (2012).
[5]M. Vukobratović and B. Borovac, "Zero-moment point—thirty five years of its life," Int. J. Humanoid Robotics **1**, 157–173 (2004).
[6]B. Siciliano and O. Khatib, *Springer Handbook of Robotics* (Springer, 2016).
[7]G. Taga, "A model of the neuro-musculo-skeletal system for anticipatory adjustment of human locomotion during obstacle avoidance," Biologic. Cybernet. **78**, 9–17 (1998).
[8]H. Kimura, Y. Fukuoka, and A. H. Cohen, "Adaptive dynamic walking of a quadruped robot on natural ground based on biological concepts," Int. J. Robot. Res. **26**, 475–490 (2007).
[9]A. J. Ijspeert, "Central pattern generators for locomotion control in animals and robots: A review," Neural Netw. **21**, 642–653 (2008).
[10]S. L. Hooper, "Central pattern generators," Curr. Biol. **10**(5), R176–R179 (2000).
[11]M. Rabinovich, A. Selverston, L. Rubchinsky, and R. Huerta, "Dynamics and kinematics of simple neural systems," Chaos **6**, 288–296 (1996).
[12]M. Lodi, A. L. Shilnikov, and M. Storace, "Design principles for central pattern generators with preset rhythms," IEEE Trans. Neural Networks Learn. Syst. **31**(9), 3658–3669 (2019).
[13]P. A. Guertin, "The mammalian central pattern generator for locomotion," Brain Res. Rev. **62**, 45–56 (2009).
[14]J. Duysens and H. W. Van de Crommert, "Neural control of locomotion; part 1: The central pattern generator from cats to humans," Gait Posture **7**, 131–141 (1998).
[15]M. L. Shik, "Control of walking and running by means of electrical stimulation of the midbrain," Biophysics **11**, 659–666 (1966).
[16]H. Cruse, "What mechanisms coordinate leg movement in walking arthropods?," Trends Neurosci. **13**, 15–21 (1990).
[17]H. Kimura, S. Akiyama, and K. Sakurama, "Realization of dynamic walking and running of the quadruped using neural oscillator," Autonomous Robots **7**, 247–258 (1999).
[18]Y. Fukuoka, H. Kimura, and A. H. Cohen, "Adaptive dynamic walking of a quadruped robot on irregular terrain based on biological concepts," Int. J. Robot. Res. **22**, 187–202 (2003).
[19]H. Yu, H. Gao, and Z. Deng, "Enhancing adaptability with local reactive behaviors for hexapod walking robot via sensory feedback integrated central pattern generator," Robot. Autonomous Syst. **124**, 103401 (2020).
[20]Ö. Ekeberg, "A combined neuronal and mechanical model of fish swimming," Biologic. Cybernet. **69**, 363–374 (1993).
[21]S. Manzoor and Y. Choi, "Central pattern generator based motion control of hopping robot for ground level acclimatization," Int. J. Robot. Automation **35**, 43–52 (2020).
[22]L. Righetti and A. J. Ijspeert, "Pattern generators with sensory feedback for the control of quadruped locomotion," in *2008 IEEE International Conference on Robotics and Automation* (IEEE, 2008), pp. 819–824.
[23]Y. Hu, J. Liang, and T. Wang, "Parameter synthesis of coupled nonlinear oscillators for cpg-based robotic locomotion," IEEE Trans. Industr. Electron. **61**, 6183–6191 (2014).
[24]A. C. de Pina Filho, M. S. Dutra, and L. S. Raptopoulos, "Modeling of a bipedal robot using mutually coupled rayleigh oscillators," Biologic. Cybernet. **92**, 1–7 (2005).
[25]L. Xu and Q. Fu, "Design and development of a rayleigh oscillator-based reference angle generator for motion control of smart prosthetic knees," IEEE Access **8**, 32421–32431 (2020).
[26]C. Liu, Q. Chen, and J. Zhang, "Coupled Van der Pol oscillators utilised as central pattern generators for quadruped locomotion," in *2009 Chinese Control and Decision Conference* (IEEE, 2009), pp. 3677–3682.
[27]S. Inagaki, H. Yuasa, T. Suzuki, and T. Arai, "Wave CPG model for autonomous decentralized multi-legged robot: Gait generation and walking speed control," Robot. Autonomous Syst. **54**, 118–126 (2006).
[28]A. J. Ijspeert, A. Crespi, D. Ryczko, and J.-M. Cabelguen, "From swimming to walking with a salamander robot driven by a spinal cord model," Science **315**, 1416–1420 (2007).
[29]A. J. Ijspeert, "A connectionist central pattern generator for the aquatic and terrestrial gaits of a simulated salamander," Biologic. Cybernet. **84**, 331–348 (2001).
[30]H. Kimura and Y. Fukuoka, "Biologically inspired dynamic walking of a quadruped robot on irregular terrain-adaptation at spinal cord and brain stem," in *Proceedings of the First International Symposium on Adaptive Motion of Animals and Machines* (Citeseer, 2000).
[31]W. Suliman, C. Albitar, and L. Hassan, "Optimization of central pattern generator-based torque-stiffness-controlled dynamic bipedal walking," J. Robotics **2020**, 1.
[32]K. Takeda and H. Torikai, "A novel hardware-efficient central pattern generator model based on asynchronous cellular automaton dynamics for controlling hexapod robot," IEEE Access **8**, 139609–139624 (2020).
[33]E. Aljalbout, F. Walter, F. Röhrbein, and A. Knoll, "Task-independent spiking central pattern generator: A learning-based approach," Neural Process. Lett. **51**(3), 2751–2764 (2020).
[34]A. S. Lele, Y. Fang, J. Ting, and A. Raychowdhury, "Learning to walk: Spike based reinforcement learning for hexapod robot central pattern generation," in *2020 2nd IEEE International Conference on Artificial Intelligence Circuits and Systems (AICAS)* (IEEE, 2020), pp. 208–212.
[35]J. Ting, Y. Fang, A. S. Lele, and A. Raychowdhury, "Bio-inspired gait imitation of hexapod robot using event-based vision sensor and spiking neural network," arXiv:2004.05450 (2020).
[36]L. Righetti, J. Buchli, and A. J. Ijspeert, "Dynamic hebbian learning in adaptive frequency oscillators," Physica D **216**, 269–281 (2006).
[37]J. S. Bay and H. Hemami, "Modeling of a neural pattern generator with coupled nonlinear oscillators," IEEE. Trans. Biomed. Eng. **BME-34**, 297–306 (1987).
[38]C. M. Pinto and J. T. Machado, "Fractional central pattern generators for bipedal locomotion," Nonlinear Dyn. **62**, 27–37 (2010).
[39]R. Kukillaya, J. Proctor, and P. Holmes, "Neuromechanical models for insect locomotion: Stability, maneuverability, and proprioceptive feedback," Chaos **19**, 026107 (2009).
[40]S. Jalil, D. Allen, J. Youker, and A. Shilnikov, "Toward robust phase-locking in melibe swim central pattern generator models," Chaos **23**, 046105 (2013).
[41]T. Zielińska, "Coupled oscillators utilised as gait rhythm generators of a two-legged walking machine," Biologic. Cybernet. **74**, 263–273 (1996).
[42]M. S. Dutra, A. C. de Pina Filho, and V. F. Romano, "Modeling of a bipedal locomotor using coupled nonlinear oscillators of Van der Pol," Biologic. Cybernet. **88**, 286–292 (2003).
[43]S. Astakhov, O. Astakhov, V. Astakhov, and J. Kurths, "Bifurcational mechanism of multistability formation and frequency entrainment in a Van der Pol oscillator with an additional oscillatory circuit," Int. J. Bifurcat. Chaos **26**, 1650124 (2016).
[44]B. Ermentrout, *Simulating, Analyzing, and Animating Dynamical Systems: A Guide to XPPAUT for Researchers and Students* (SIAM, 2002).
[45]V. Anishchenko, S. Astakhov, and T. Vadivasova, "Phase dynamics of two coupled oscillators under external periodic force," Europhys. Lett. **86**, 30003 (2009).
[46]J. Rose and J. G. Gamble, *Human Walking* (Williams & Wilkins, 1994).
[47]D. A. Winter, "Biomechanical motor patterns in normal walking," J. Motor Behav. **15**, 302–330 (1983).
[48]A. Bahramian, A. Nouri, F. Towhidkhah, H. Azarnoush, and S. Jafari, "Introducing a nonlinear coupling for central pattern generator: Improvement on robustness by expanding basin of attraction and performance by decreasing the transient time," J. Vibration Control **26**, 377–386 (2020).
[49]S. Aoi, D. Katayama, S. Fujiki, N. Tomita, T. Funato, T. Yamashita, K. Senda, and K. Tsuchiya, "A stability-based mechanism for hysteresis in the walk–trot transition in quadruped locomotion," J. R. Soc. Interface **10**, 20120908 (2013).
[50]M. Abdolvahab, "A synergetic model for human gait transitions," Physica A. **433**, 74–83 (2015).
[51]J. Shan, C. Junshi, and C. Jiapin, "Design of central pattern generator for humanoid robot walking based on multi-objective Ga," in *Proceedings. 2000 IEEE/RSJ International Conference on Intelligent Robots and Systems (IROS 2000)(Cat. No. 00CH37113)* (IEEE, 2000), Vol. 3, pp. 1930–1935.